Open access • Journal Article • DOI:10.1016/J.PRP.2017.09.022

3D modelling of radical prostatectomy specimens: Developing a method to quantify tumor morphometry for prostate cancer risk prediction — Source link

Marcus C. Hovens, Kevin Lo, Michael Kerger, John Pedersen ...+8 more authors

Institutions: University of Queensland, Royal Melbourne Hospital, Monash University, Clayton campus

Published on: 27 Sep 2017 - Pathology Research and Practice (Elsevier)

Topics: Prostate neoplasm, Prostate cancer, Prostatectomy, Prostate-specific antigen and Prostate

Title: 3D modelling of radical prostatectomy specimens: developing a method to quantify tumor morphometry for prostate cancer risk prediction

Authors: Marcus C. Hovens, Kevin Lo, Michael Kerger, John Pedersen, Timothy Nottle, Natalie Kurganovs, Andrew Ryan, Justin S. Peters, Daniel Moon, Anthony J. Costello, Niall M. Corcoran, Matthew K.H. Hong

PII: S0344-0338(17)30817-8
DOI: https://doi.org/10.1016/j.prp.2017.09.022
Reference: PRP 51903

To appear in:

Received date: 10-8-2017
Revised date: 18-9-2017
Accepted date: 18-9-2017

Please cite this article as: Marcus C.Hovens, Kevin Lo, Michael Kerger, John Pedersen, Timothy Nottle, Natalie Kurganovs, Andrew Ryan, Justin S.Peters, Daniel Moon, Anthony J.Costello, Niall M.Corcoran, Matthew K.H.Hong, 3D modelling of radical prostatectomy specimens: developing a method to quantify tumor morphometry for prostate cancer risk prediction, Pathology - Research and Practice https://doi.org/10.1016/j.prp.2017.09.022

3D modelling of radical prostatectomy specimens: developing a method to quantify tumor morphometry for prostate cancer risk prediction

Marcus C. Hovens [c], Kevin Lo[a], Michael Kerger[a], John Pedersen [b], Timothy Nottle [b], Natalie Kurganovs[a], Andrew Ryan [b], Justin S. Peters[a], Daniel Moon[a], Anthony J. Costello[a], Niall M. Corcoran[a*] and Matthew K.H. Hong[a],

[a] Division of Urology, Department of Surgery, Royal Melbourne Hospital, University of Melbourne, Parkville and Australian Prostate Cancer Research Centre at Epworth Hospital, Richmond, VIC, Australia

[b] TissuPath Specialist Pathology, Mount Waverley and the Faculty of Medicine, Monash University, Clayton, VIC, Australia

[c] School of Medicine, University of Queensland, St Lucia, QLD, Australia

*Corresponding Author: Dr Niall Corcoran, Department of Surgery, 5th Floor Clinical Sciences Bldg, Royal Melbourne Hospital, University of Melbourne, Parkville, 3050, VIC Australia.

Phone: +613 9342 7703

Fax: +613 9347 6488

Email: con@unimelb.edu.au

Abstract

Prostate cancer displays a wide spectrum of clinical behaviour from biological indolence to rapidly lethal disease, but we remain unable to accurately predict an individual tumor's future clinical course at an early curable stage. Beyond basic dimensions and volume calculations, tumor morphometry is an area that has received little attention, as it requires the analysis of the prostate gland and tumor foci in three-dimensions. Previous efforts to generate three-dimensional prostate models have required specialised graphics units and focused on the spatial distribution of tumors for optimisation of biopsy strategies rather than to generate novel morphometric variables such as tumor surface area. Here, we aimed to develop a method of creating three-dimensional models of a prostate's pathological state post radical prostatectomy that allowed the derivation of surface areas and volumes of both prostate and tumors, to assess the method's accuracy to known clinical data, and to perform initial investigation into the utility of morphometric variables in prostate cancer prognostication. Serial histology slides from 21 prostatectomy specimens covering a range of tumor sizes and pathologies were digitised. Computer generated three-dimensional models of tumor and prostate space filling models were reconstructed from these scanned images using Rhinoceros 4.0 spatial reconstruction software. Analysis of three-dimensional modelled prostate volume correlated only moderately with weak concordance to that from the clinical data ($r=0.552$, $\theta=0.405$), but tumor volume correlated well with strong concordance ($r=0.949$, $\theta=0.876$). We divided the cohort of 21 patients into those with features of aggressive tumor versus those without and found that larger tumor surface area (32.7 vs 3.4cc, $p=0.008$) and a lower tumor surface area to volume ratio (4.7 vs 15.4, $p=0.008$) were associated with aggressive tumor biology.

Key words: Prostate cancer, radical prostatectomy, histopathology, tumor spatial reconstruction, 3 dimensional modelling,

1. Introduction

Prostate cancer is now the most commonly diagnosed internal malignancy in the Western world. Unlike other cancers, prostate cancer displays a wide spectrum of clinical behaviour from biological indolence to rapidly lethal disease. However, the ability to accurately predict the future clinical course of any individual tumor at an early curable stage remains elusive [12]. In the setting of a genomics revolution and a plethora of new prognostic molecular tests for prostate cancer [2, 8, 11], one area that has remained largely unexplored is that of tumor morphometry. Whereas macroscopic tumor measurements have long been used in the study of cancer and correlated with clinical outcomes, factors such as tumor surface area or shape, or even the surface area of extraprostatic extension have been much more difficult to quantify and incorporate into statistical models that might help to predict future clinical behaviour. Within current clinical practice, tumor shape at best would be a highly subjective categorical variable. However, a surrogate marker for this could be the ratio of tumor surface area to volume, as this would tend to increase with more complex tumor shapes that might correlate with more aggressive phenotypes. Whilst tumor volume can be inferred by simple planimetry of series of two dimensional histology slides, in order to measure surface area, one must convert data from two-dimensional histological slides into a three-dimensional construct that can then be analysed.

The advent of readily available graphics processing and three-dimensional rendering have allowed previous researchers to utilise 3D software in the study of prostate cancer [1, 3, 4, 10, 13-15]. However, these previous reports have created 3D renditions of prostate glands focussing specifically on the spatial distribution of individual tumor foci with the intention of improving biopsy strategies and required large specialised graphics systems, or utilised other

not readily accessible, imaging modalities such as MRI as a framework to build and validate the models.

The recent introduction of MRI into the clinical management of prostate cancer offers images of both prostate gland and tumor foci, although these can still be difficult to define [9]. Three-dimensional reconstruction from radiological modalities is not new, and the future analysis of tumor morphometry from this new imaging modality is likely.

However, clinical databases incorporating MRI data are far from mature in that long term outcomes are not yet known, and there exist many more prostatectomy databases linked with archival tissues from which surgical and oncological outcomes are known. A study of the three-dimensional properties of prostate cancer could provide prognostic information for prostate cancer or valuable insight into how MRI could inform surgical resectability. To this end, we aimed to develop using standard desktop computers a method of accurate 3D modelling of prostate glands and their tumors using archival tissue available in contemporary clinical practice to derive morphometric measures, namely tumor volume and surface area, and validate these where possible against known values from clinicopathological data. In an exploratory analysis, we then examined the novel morphometric variables of tumor surface area and surface area to volume ratio as factors in our cohort divided into groups based on known markers of prostate cancer aggression.

2. Materials and Methods

2.1 Clinical Data Source

We accessed a clinical database of over 800 patients who underwent robotic prostatectomy at our institution from the period 2003 to 2008, with a median follow-up of more than three years [6]. The information in this database included a wide range of clinico-pathological variables including age, preoperative PSA level, and postoperative PSA levels recorded during follow-up. Institutional review board approval was obtained. Pathology data from the final prostatectomy specimen were also recorded, and included Gleason scores, pathological tumor stage (pT stage), seminal vesical involvement (SVI), extraprostatic extension (EPE), focality and surgical margins (SM). Prostate volume and tumor volume data were included also.

2.2 Digitisation of 2D Histology Data

Following prostatectomy, specimens were routinely fixed in their entirety in formalin and blocked in paraffin [5]. Transverse sections at 5 mm intervals were then made perpendicular to the urethra from apex to base, throughout the entire specimen. A 5μm slice was then subsequently made from each section, stained with haematoxylin and eosin and both prostate and tumor borders marked by different coloured pens. These slides consisted of horizontal sections taken 5mm apart from base to apex, with vertical sections taken at varying thicknesses at the base and apex and placed alongside. Where involved with disease, the seminal vesicles were also included in these slides with areas of tumor marked. Each marked tissue section was digitally scanned and images recorded in Adobe Photoshop in .jpg format.

2.3 Prostate and Tumor 3D reconstruction

A method for converting 2D histology information into 3D models was developed and refined using multiple test cases after a period of familiarisation with the software. Adobe Photoshop was used to draw separate paths around each tumor group and the prostate outline on each histology slide. These paths were imported into Rhinoceros 4.0 with the grid adjusted such that each square represented 5mm. Both the tumor and prostate paths were simplified by creating new continuous curves around each object. Each curve corresponding to vertical slices was rotated 90° and aligned to sit atop the end horizontal slices. The segments of each individually refined arch were then "Joined" to form into a series of loftable arches.

The same process was applied to each of the individual tumors to develop a loftable skeleton. Prostate and tumor outlines were then transformed into a 3-dimensional drape created by lofting. This process was performed for the entire prostate both vertically and horizontally, thus creating the full outer shape in three dimensions. All surfaces for the prostate drape were then joined to the selected objects to create a single closed polysurface, to complete the prostate model. As tumor shape was far more variable than that of the prostate, subjective assessment of predicted tumor shapes were made to guide selection of outlines and loft joins between histopathological slices.

A series of 21 cases covering a diverse range of pathologies as well as prostate and tumor shapes were then selected for modelling with the developed protocol. Validation of the modelling technique was by way of comparison to the original clinical data, whilst a pilot analysis of the novel variables of surface area to volume ratio in different cohorts was also undertaken. Histology slides for radical prostatectomy specimens for each case were obtained and scanned as above and three-dimensional models created with the protocol. Modelling was conducted blind to all clinciopathological data. The surface area and volume calculations of each object were extracted within Rhinoceros 4.0 and tabulated.

2.4 Validation of 3D Model Derived Variables

Spearman's rank-order correlation coefficient was used to assess for correlation between the values derived from the 3-D model and the corresponding clinicopathological values including prostate and tumor volumes, margin positivity and extraprostatic extension, and multifocality. Original tumor volumes had been calculated from the source clinical data using NIH image as previously described [5]. Briefly, measured tumor areas on the slides were totalled and using an assumed section thickness of 5mm, tumor volume was calculated through planimetry. Accuracy of variables derived from 3D models to that from the clinicopathological data were compared using Bland-Altman plots and Lin's concordance coefficient.

2.5 Pilot Study

We divided the cohort of 21 patients into those with smaller less aggressive tumors with no recurrence (n=12) versus those with larger more aggressive tumors (n=9) and analysed for differences between morphometric variables including surface area, volumes and surface area to volume ratio.

2.6 Statistical Analysis

The Mann-Whiney U test was used in assessing the continuous data, deemed non-normally distributed by tests of normality. We analysed all data with PASW Statistics 18.0 (formerly SPSS, Chicago, IL, USA). All statistical tests were two-sided with significance assumed at p values <0.05.

3. Results

Three-dimensional models for radical prostatectomy specimens were constructed for a total of twenty-one individual cases and variables derived and tabulated from these models **(Table 1)**. We began with validation of the accuracy to clinical references of the values derived from these 3D models including the physical characteristics of prostate volume and tumor volume, and the pathological features of margin positivity, extraprostatic extension and tumor multifocality.

3.1 Accuracy to measured prostate volume

The mean prostate volume derived from the 3-D models (29.5±8.7cc) was slightly lower than that derived from clinical data (35.8±16.7cc). Spearman rank-order correlation coefficient showed moderate correlation between the variables (Spearman's rho=0.552, p=0.009) (**Fig 1**). Given that prostate weight is a more accurate reflection of the size of the prostate, as prostate volume is derived from ultrasound rather than histological measurements [7], we then correlated the prostate volumes with the measured prostate weights from the clinical data to show a slightly higher correlation (Spearman's rho=0.633, p=0.002).

Bland-Altman analysis between the prostate volume variables derived from the two different sources revealed a bias of 10.3cc (-23.9 to 44.6, 95% CI) in the data derived from the 3D models, with relatively low concordance of 0.405 (0.24 to 0.54).

3.2 Accuracy to measured tumor volume

Comparison of tumor volumes derived from 3D models versus clinical data yielded much greater correlation (Spearman's rho=0.949, p <0.001). Bland-Altman plot showed a bias of 1.93cc (-2.7 to 6.4, 95% CI) towards the 3D derived values and concordance coefficient was strong at 0.876 (0.80 to 0.92), suggesting that the tumor volumes calculated through the 3D

modelling process was accurate to the tumor volumes from the clinical data for this cohort (**Fig 2**).

3.3 Accuracy to margin positivity and extraprostatic extension

On changing the view settings to "Shaded", the 3-D models had the ability to show visually in virtual 3-D space any positive margins or extraprostatic extension (EPE) if present, although limited in its ability to differentiate between the two (**Fig 3, Fig 4A, 4B**). Models were assessed on whether or not any positive margins or EPE were visible in the model, that is, if the modelled tumor was "organ confined", and whether this correlated with the source clinical data. We also assessed whether the positive margins corresponded to the correct physical locale with reference to the original histological slides. This was performed on each of the 21 3D models by retrospective visual inspection. It was noted that if the tumor was located right on the periphery of the prostate but was not microscopically margin positive, a few slivers of the tumor drape could still show through the prostate drape to show this shared border, but not enough to denote the finding on the 3-D model (**Fig 3**).

3.4 Accuracy to multifocality

Multifocality in the models was compared to multifocality in the clinical data, and all but two of the models in this cohort (cases 14 and 16) correlated with the clinical data in this respect. The two cases that did not correlate showed multifocality in the 3-D model when the clinical data was noted to be unifocal.

3.5 Analysis of morphometric variables in the discovery cohort

We next explored the morphometric variables for which no gold standard in clinical data existed, including tumor surface area, and surface area to volume ratio that was a surrogate for tumor shape. The cohort was divided into non-aggressive versus aggressive groups.

The total tumor surface area was much smaller in the non-aggressive group compared with the aggressive group with medians [quartiles] of 3.44 [1.7, 12.3] and 32.7 [28.2, 43.0] cm² respectively (p=0.008). We next examined prostate shape as measured by the surrogate variable of prostate surface area to volume ratio. As expected, there was no apparent difference between the two groups with medians [quartiles] of 1.95 [1.8, 2.0] and 1.91 [1.8, 2.0] cm^2 for non-aggressive and aggressive groups respectively (p=0.968). Finally, we examined tumor shape as measured by the surrogate variable of total tumor surface area to volume. Interestingly, this ratio was significantly larger in the non-aggressive group compared with the aggressive group with medians [quartiles] of 15.40 [9.9, 18.4] and 4.73 [3.1, 5.9] respectively (p=0.008).

4. Discussion

In this study we have developed a method to construct 3D models of prostatectomy specimens across a range of tumor sizes and pathologies. From these models we derived basic morphometric measurements including prostate and tumor volumes and compared this with known values from the clinical data. We next derived previously inelicitable novel variables such as tumor surface area and demonstrated how this might be studied for prognostic ability in a patient cohort divided by tumor aggression.

Previous reports of 3D prostate models have not validated against known clinical data as they have been aimed at tumor location for improving biopsy targeting [1-3, 10, 14, 15]. Nevertheless, compared to the clinical data, our 3D model derived tumor volume showed strong correlation and concordance ($r=0.949$, $\theta=0.876$). The accuracy could be explained by the planimetry used for the generation of original tumor volume measurements in the clinical dataset. In contrast, 3D model derived prostate volume demonstrated only a moderate

relationship with poorer concordance with similar measures from the clinical dataset (r=0.552, θ=0.405). The original prostate volumes were calculated by applying the prolate ellipsoid formula to three measured dimensions from the pathology specimens, that is the prostate was mathematically modelled as an ellipse [7]. Indeed, examination of our 3D models showed that prostate shape was far more variable, and as these models were based purely from the theoretically more accurate scale images depicting the radical prostatectomy specimens, there is the possibility that these model derived values were closer to the true volumes than the formula derived approximations. Of note, correlation improved when model derived prostate volume was compared against the more accurate measure of prostate weight [7].

The analysis using the novel morphometric variables showed promise. As this was a secondary aim and the study size limited to a pilot group selected more for a range of tumor sizes, only very limited inferences can be made. Tumor surface area was much larger in the aggressive tumor group at median 32.7cc compared with just 3.4cc (p=0.008), but this was in keeping with the extreme disparity between the groups in terms of tumor grade, local tumor stage and biochemical outcome, that is the aggressive group had larger tumors. Using tumor surface area to volume ratio as a proxy for tumor shape yielded a higher ratio in the non-aggressive group (15.4 vs 4.73, p=0.008), meaning a greater deviation from a perfect sphere that might be associated with more aggressive morphology. This is a curious result, but the extreme differences in tumor volume and differences in multifocality within the limited could account for this. A further study with a larger cohort and more precisely defined tumor factors would be required to more fully evaluate this ratio in a prognostic capacity.

The limitations of our 3D modelling technique include the labour intense nature of computer graphics work, the subjective assessment required at times and the limitations imposed by the 5mm sectioning interval at the original pathology processing in that the models are still dependent on interpolation between sections. In addition, the clinical cohort was small and

retrospectively sampled. On the other hand, we have demonstrated a relatively simple process that requires only a desktop computer and no special requirements of the radical prostatectomy specimen processing. This allows the modelling method to be applied across large archives of radical prostatectomy specimens linked with outcomes data without restriction. We are now in the process of exploring prostate cancer morphometry and its influence on pathology and oncological outcomes amongst our radical prostatectomy cohort.

In conclusion, we have developed an accurate method of modelling in three dimensions the prostate gland with tumor foci from radical prostatectomy specimens and derived novel morphometric tumor variables. Further study of these variables as prognostic factors is required in larger more specifically defined cohorts.

5. Conclusions

We have developed a three-dimensional modelling technique for radical prostatectomy specimens, from which we were able to derive morphometric tumor measurements such as surface area, applicable to common archival prostatectomy tissue, and which could be used in a small pilot study of prostate cancer prognosis. Further investigation of these new variables with larger more precisely defined cohorts will be required to validate the utility of 3D modelling as a prognostic tool.

.

Ethical approval

The study obtained Institutional Review Board approval. This article does not contain any animal studies performed by any of the authors.

Informed consent

Informed consent for research was obtained by all participants in the study.

Conflict of interest

The authors declare no conflict of interest

Acknowledgments

M.K.H.H. was supported by scholarships from the National Health and Medical Research Council, Australia, University of Melbourne (Melville Hughes Scholarship) and the Royal Australasian College of Surgeons (Foundation of Surgery Catherine Marie Enright Kelly and ANZ Journal of Surgery Research Scholarships). N.M.C. is the recipient of a David Bickart Clinician Research Fellowship from the Faculty of Medicine, Dentistry and Health Sciences at the University of Melbourne. M.K. was supported by the Carlo Vaccari Scholarship and APCR. This work was supported in part by NHMRC project grants 1024081 (N.M.C., J.S.P., A.J.C. and C.M.H.) and 1047581 (C.M.H., G.M., I.H., J.S.P., A.J.C., N.M.C.), as well as a federal grant from the Australian Department of Health and Aging to the Epworth Cancer Centre, Epworth Hospital (A.J.C., N.M.C., C.M.H.).

References

[1] J.J. Bauer, J. Zeng, J. Weir, W. Zhang, I.A. Sesterhenn, R.R. Connelly, S.K. Mun, J.W. Moul, Three-dimensional computer-simulated prostate models: lateral prostate biopsies increase the detection rate of prostate cancer. Urology 53 (1999) 961-967.

[2] J. Cullen, I.L. Rosner, T.C. Brand, N. Zhang, A.C. Tsiatis, J. Moncur, A. Ali, Y. Chen, D. Knezevic, T. Maddala, H.J. Lawrence, P.G. Febbo, S. Srivastava, I.A. Sesterhenn, D.G. McLeod, A Biopsy-based 17-gene Genomic Prostate Score Predicts Recurrence After Radical Prostatectomy and Adverse Surgical

Pathology in a Racially Diverse Population of Men with Clinically Low- and Intermediate-risk Prostate Cancer. Eur Urol 68 (2015) 123-131.

[3] L. Egevad, H. Frimmel, M. Norberg, S. Mattson, I. Carlbom, E. Bengtsson, C. Busch, Three-dimensional computer reconstruction of prostate cancer from radical prostatectomy specimens: evaluation of the model by core biopsy simulation. Urology 53 (1999) 192-198.

[4] E. Gibson, M. Gaed, J.A. Gomez, M. Moussa, C. Romagnoli, S. Pautler, J.L. Chin, C. Crukley, G.S. Bauman, A. Fenster, A.D. Ward, 3D prostate histology reconstruction: an evaluation of image-based and fiducial-based algorithms. Med Phys 40 (2013) 093501.

[5] M.K. Hong, B. Namdarian, N.M. Corcoran, J. Pedersen, D.G. Murphy, J.S. Peters, L. Harewood, N. Sapre, K. Rzetelski-West, A.J. Costello, C.M. Hovens, Prostate tumour volume is an independent predictor of early biochemical recurrence in a high risk radical prostatectomy subgroup. Pathology 43 (2011) 138-142.

[6] M.K. Hong, H.H. Yao, J.S. Pedersen, J.S. Peters, A.J. Costello, D.G. Murphy, C.M. Hovens, N.M. Corcoran, Error rates in a clinical data repository: lessons from the transition to electronic data transfer--a descriptive study. BMJ Open 3 (2013).

[7] M.K. Hong, H.H. Yao, K. Rzetelski-West, B. Namdarian, J. Pedersen, J.S. Peters, C.M. Hovens, N.M. Corcoran, Prostate weight is the preferred measure of prostate size in radical prostatectomy cohorts. BJU Int 109 Suppl 3 (2012) 57-63.

[8] M. Marrone, A.L. Potosky, D. Penson, A.N. Freedman, A 22 Gene-expression Assay, Decipher(R) (GenomeDx Biosciences) to Predict Five-year Risk of Metastatic Prostate Cancer in Men Treated with Radical Prostatectomy. PLoS Curr 7 (2015).

[9] F.V. Mertan, M.D. Greer, J.H. Shih, A.K. George, M. Kongnyuy, A. Muthigi, M.J. Merino, B.J. Wood, P.A. Pinto, P.L. Choyke, B. Turkbey, Prospective Evaluation of the Prostate Imaging Reporting and Data System version 2 (PI-RADSv2) for Prostate Cancer Detection. J Urol (2016).

[10] M.B. Opell, J. Zeng, J.J. Bauer, R.R. Connelly, W. Zhang, I.A. Sesterhenn, S.K. Mun, J.W. Moul, J.H. Lynch, Investigating the distribution of prostate cancer using three-dimensional computer simulation. Prostate Cancer Prostatic Dis 5 (2002) 204-208.

[11] S. Roychowdhury, A.M. Chinnaiyan, Advancing precision medicine for prostate cancer through genomics. J Clin Oncol 31 (2013) 1866-1873.

[12] Y. Shieh, M. Eklund, G.F. Sawaya, W.C. Black, B.S. Kramer, L.J. Esserman, Population-based screening for cancer: hope and hype. Nat Rev Clin Oncol (2016).

[13] P.N. Werahera, G.J. Miller, K. Torkko, E.D. Crawford, J.S. Stewart, E.P. Deantoni, H.L. Miller, M.S. Lucia, Biomorphometric analysis of human prostatic carcinoma by using three-dimensional computer models. Hum Pathol 35 (2004) 798-807.

[14] J. Zeng, J. Bauer, S.K. Mun, Modeling and mapping of prostate cancer. Computers & Graphics 24 (2000) 683-694.

[15] J. Zeng, J. Bauer, W. Zhang, I. Sesterhenn, R. Connelly, J. Lynch, J. Moul, S.K. Mun, Prostate biopsy protocols: 3D visualization-based evaluation and clinical correlation. Comput Aided Surg 6 (2001) 14-21.

Figures

Figure 1. Comparison of prostate volume calculated from 3-D model with **(A)** prostate volume derived from measurements from clinical data and **(B)** prostate weight also from clinical data. **(C)** Bland Altman plot of concordance between prostate volume measures.

Figure 2. **(A)** Comparison of the total tumour volume derived from the 3-D model with that from the clinical data. **(B)** Bland-Altman plot of concordance between tumour volume measures.

Figure 3. Images from 2-D pathology slides (above) from which prostate glands with their tumours were modelled in 3-D (below) and showing cases where (A) the tumour was organ-confined as can be seen in the 3-D model below; (B) extraprostatic extension and multifocality with tumour clearly extending beyond the modelled prostate (red).

Figure 4. Alternative views of a prostate (green) with extracapsular extension tumours (red) modelled in 3-D with side on view in (A) and superior view in (B).

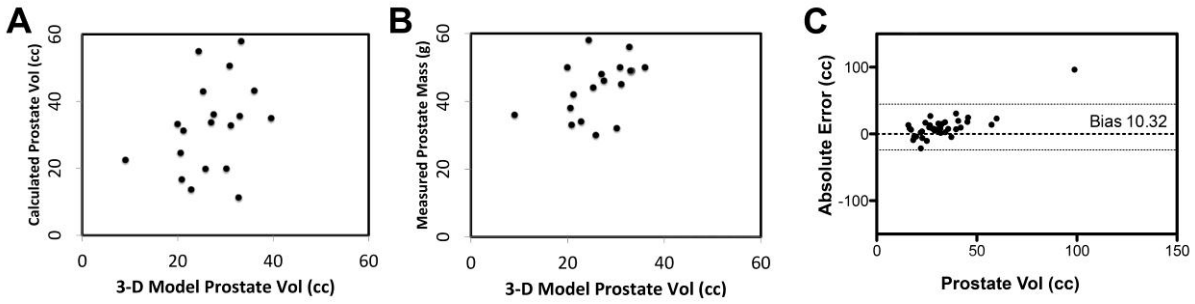

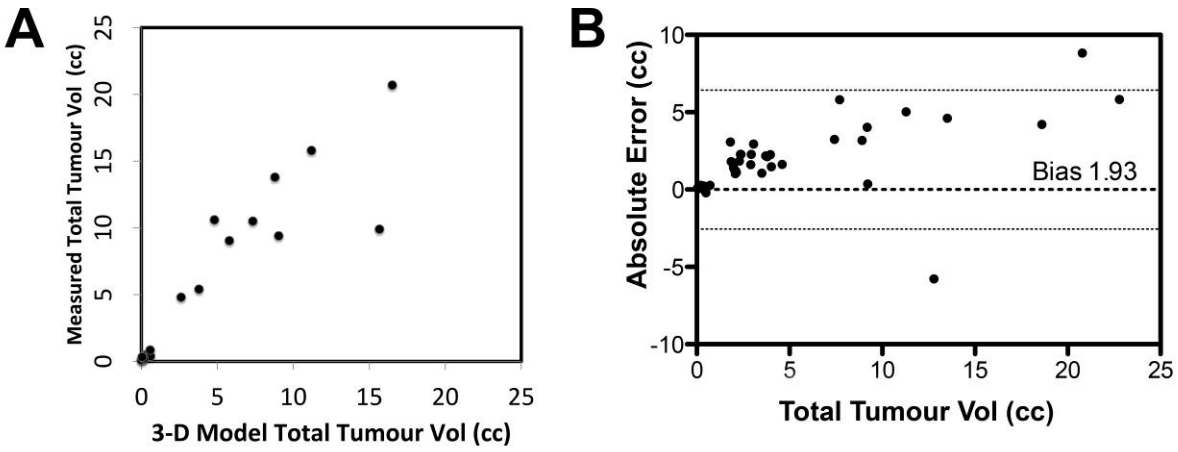

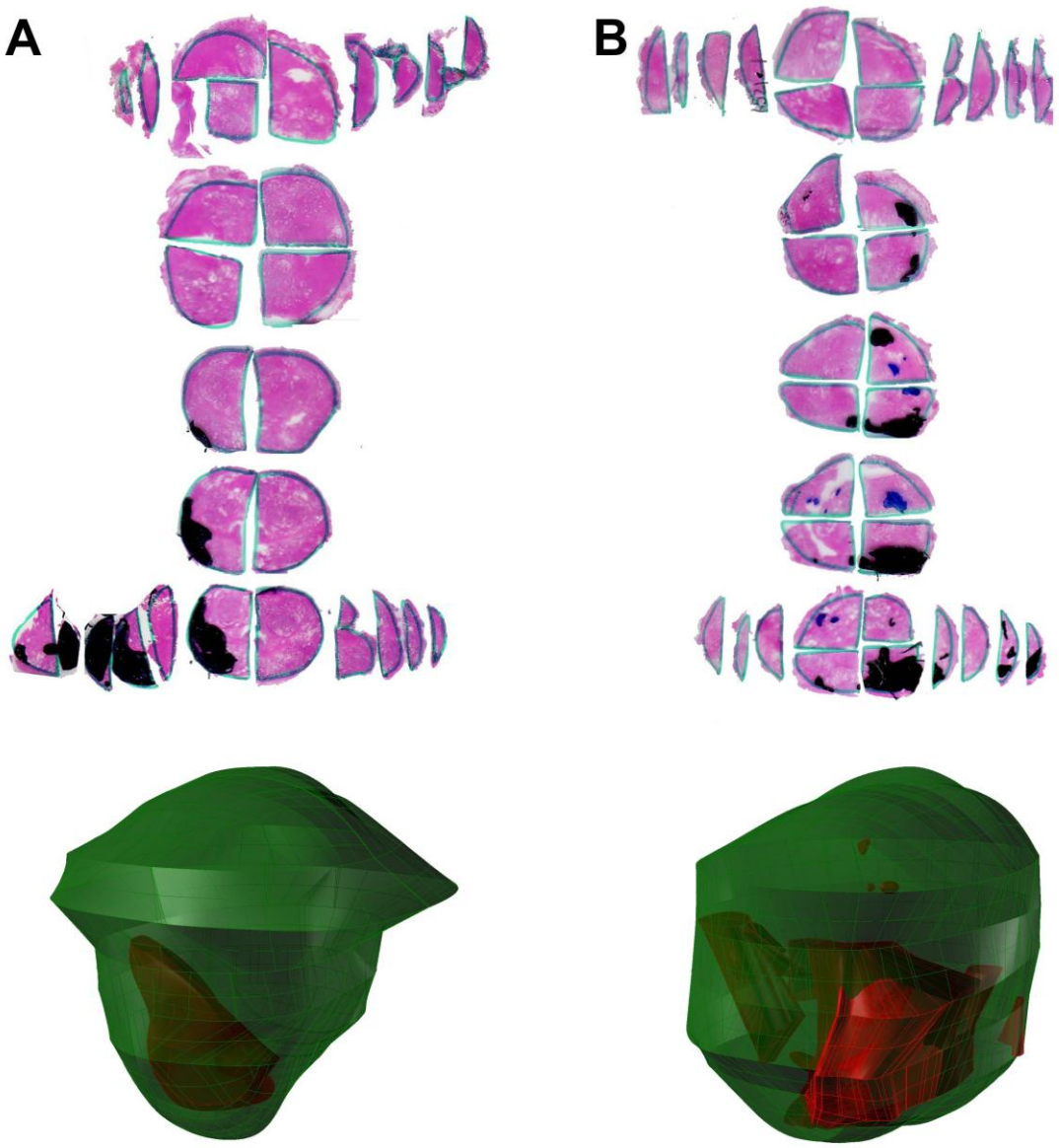

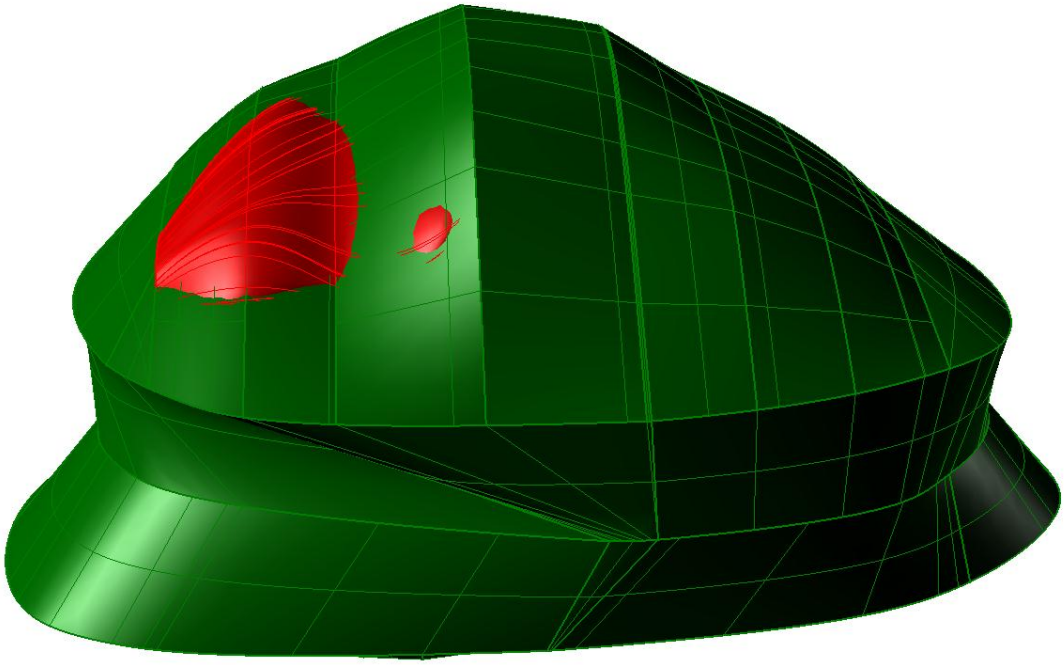

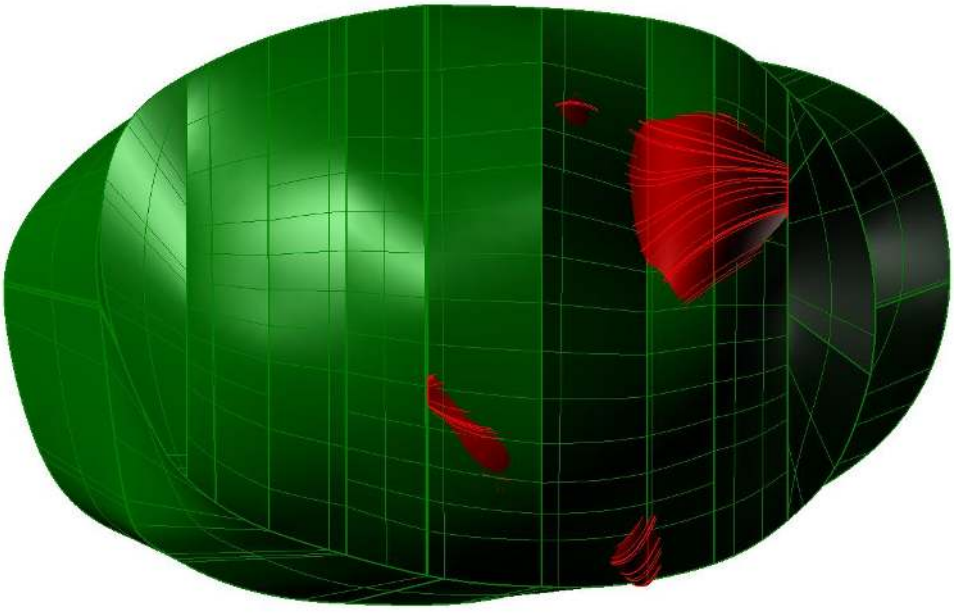

	Derived from 3D Model													**From Clinical Data**								
	Prostate		Tumour 1		Tumour 2		Tumour 3		**Total Tumour**													
	Surface Area (cm^2)	**Vol (cc)**	**Surface Area (cm^2)**	**Vol (cc)**	**Surface Area (cm^2)**	**Vol (cc)**	**Surface Area (cm^2)**	**Vol (cc)**	**Surface Area (cm^2)**	**Vol (cc)**	**Prostate SA: Vol**	**Total tumour SA:Vol**	**Prostate vol:total tumour vol**	**Prostate Vol (cc)**	**Prostate Mass (g)**	**Peripheral Tumour Vol**	**TZ Tumour Vol**	**Gleason Score**	**Staging**	**Multifocal**	**EPE**	**Recurrence***
1	54.45	31.14	27.96	9.04					27.96	9.04	1.75	3.09	3.44	32.8	45	9.4		3+3 SMS+	pT2c	No	No	No Recurrence (3 years)
2	52.78	27.04	2.2	0.13	1.36	0.1	0.8	0.046	4.36	0.28	1.95	15.80	97.97	33.7	48	0.4	0.1	3+3 SMS-	pT2c	Yes	No	No Recurrence (2 years)
3	38.91	9.07	1	0.06	0.14	0.002	0.129	0.002	1.27	0.06	4.29	19.83	141.72	22.5	36		0.2	3+3 SMS-	pT2c	Yes	No	No Recurrence (2 years)
4	47.29	24.40	2.25	0.15					2.25	0.15	1.94	15.00	162.67	54.9	58	0.4		3+3 SMS-	pT2a	No	No	No Recurrence (2 years)
5	61.15	33.32	0.95	0.053					0.95	0.05	1.84	17.92	628.70	57.9	49	0.24		3+3 SMS-	pT2a	No	No	No Recurrence (3 years)
6	43.97	19.97	0.039	0.00045					0.04	0.00	2.20	86.67	44377.78	33.2	50	0.09		3+3 SMS-	pT2a	No	No	No Recurrence (2 years)
7	50.51	25.32	6.81	0.603					6.81	0.60	1.99	11.29	41.99	42.9	44	0.39		3+3 SMS-	pT2c	No	No	No Recurrence (2 years)
8	51.08	27.54	9.4	1.372	36.08	9.828			45.48	11.20	1.85	4.06	2.46	36.0	46	15.8		4+5 SMS+	pT3b	No	Yes	No Recurrence (3 years)
9	54.97	32.78	24.9	4.309	25.14	4.472			50.04	8.78	1.68	5.70	3.73	11.2	56	6.3	7.5	3+4 SMS+	pT2c	Yes	No	No Recurrence (2 years)
10	74.32	50.38	2.38	0.146	0.13	0.0025			2.51	0.15	1.48	16.91	339.34	64.4	72	0.22		3+3 SMS-	pT2c	Yes	No	No Recurrence (4 years)
11	42.87	20.85	1.43	0.042	0.42	0.017			1.85	0.06	2.06	31.36	353.32	16.6	33	0.34		3+3 SMS-	pT2a	Yes	No	No Recurrence (3 years)
12	44.93	21.24	4.62	0.393	2.47	0.183	0.013	0.002	7.10	0.58	2.12	12.29	36.75	31.2	42	0.27	0.58	3+3 SMS-	pT2c	Yes	No	No Recurrence (3 years)
13	68.12	39.60	42.03	16.501					42.03	16.50	1.72	2.55	2.40	34.9	62	20.7		4+5 SMS+	pT3a	No	Yes	Recurrence (2 years)
14	59.59	33.03	25.2	5.626	2.23	0.17			27.43	5.80	1.80	4.73	5.70	35.6	49	9.04		4+3 SMS+	pT3b	No	Yes	Recurrence (2 years)
15	59.56	30.21	11.26	1.26	9.68	1.24	3.32	0.12	24.26	2.62	1.97	9.26	11.53	19.8	32	4.8		3+4 SMS+	pT3a	Yes	No	Recurrence (2.5 years)
16	53.02	22.84	40.29	7.85	2.62	0.2	0.019	7.62	42.93	15.67	2.32	2.74	1.46	13.7	34	9.9		4+3 SMS+	pT3b	No	Yes	Recurrence (0.5 years)
17	58.84	30.90	32.34	7.313	0.35	0.012			32.69	7.33	1.90	4.46	4.22	50.5	50	10.5		4+3 SMS+	pT3a	Yes	Yes	Recurrence (3 years)

18	72.85	48.32	60.58	19.828	0.85	0.027	0.45	0.011	61.88	19.87	1.51	3.11	2.43	71.5	65	25.7		4+5 SMS-	pT3b	Yes	Yes	Recurrence (2 years)
19	49.33	25.87	25.35	3.566	2.18	0.166	1.46	0.053	28.99	3.79	1.91	7.66	6.83	19.8	30	5.02	0.39	4+5 SMS+	pT3a	Yes	Yes	Recurrence (4 years)
20	71.36	36.04	62.14	13.544	15.29	2.822			77.43	16.37	1.98	4.73	2.20	43.2	50	25.2		5+4 SMS+	pT3b	Yes	No	Recurrence (2 years)
21	50.69	20.63	23.61	4.506	3.65	0.263	0.92	0.032	28.18	4.80	2.46	5.87	4.30	24.6	38	10.6		4+5 SMS+	pT3b	Yes	Yes	Recurrence (3 years)

Table 1. Data derived from 3D modelling compared to clinical data. *TZ* – transitional zone; *SMS* – Surgical Margin (positive or negative); *EPE* – Extraprostatic Extension. * Biochemical recurrence with either follow up in years or time to recurrence